# Microwave assisted synthesis of $MnO_2$ on Nickel Foam-Graphene for Electrochemical Capacitor

**A. Bello[1], O. O Fashedemi[2], M. Fabiane[1], J. N. Lekitima[2], K. I. Ozoemena[2,3] and N. Manyala[1*]**

[1]Department of Physics, Institute of Applied Materials, SARCHI Chair in Carbon Technology and Materials, University of Pretoria, Pretoria 0028, South Africa.
[2]Department of Chemistry, University of Pretoria, Pretoria 0002, South Africa.
[3]Council for Scientific and Industrial Research, Pretoria South Africa, Meiring Naude Road, Brummeria, 395 Pretoria, 0001, South Africa.
***Email address:** ncholu.manyala@up.ac.za (N. Manyala)
**Corresponding author.** Tel: +27 (0)12 420 3549, Fax: +27 (0)12 420 2516

## Abstract

A green chemistry approach (Hydrothermal Microwave Irradiation) has been used to deposit manganese oxide on nickel foam-graphene. The 3D graphene was synthesized using nickel foam template by chemical vapour deposition (CVD) technique. Raman spectroscopy, X-ray diffraction (XRD), scanning electron and transmission electron microscopies (SEM and TEM); have been used to characterize structure and surface morphology of the composite respectively. The Raman spectroscopy measurements on the samples reveal that 3D graphene consists of mostly few layers with low defect density. The composite was tested in a three electrode configuration for electrochemical capacitor, and exhibited a specific capacitance of 305 F $g^{-1}$ at a current density of 1 A $g^{-1}$ and showed excellent cycling stability. The obtained results demonstrate that microwave irradiation technique could be a promising approach to synthesis graphene based functional materials for electrochemical applications.

**Keywords**: Nickel foam-Graphene (NF-G), CVD, Microwave irradiation, Nanostructure $MnO_2$, Electrochemical capacitor.

## 1 Introduction

Supercapacitors are electrochemical double layer capacitors that have attracted much attention due to their high power density, long cycle life, low temperature sensitivity, low maintenance cost and environmentally friendly nature [1–3]. They fill the gap between batteries (high energy density) and electrolytic capacitors (high power density) [4]. However, the energy stored in supercapacitor

devices (<10 W h $kg^{-1}$) is low compared to batteries (>100 W h $kg^{-1}$). This has imposed significant and difficult challenges in employing supercapacitors as primary power source for battery replacement [5,6]. It has also restricted the use of supercapacitors for possible applications such as memory back-up equipment, hybrid vehicles, cordless electric tools, cellular phones and entertainment instruments [7]. Carbon materials such as activated carbon have been used as electrode material for supercapacitors. However, their poor electrochemical performance has limited them for practical applications [8]. Conducting polymers, transition metal oxide and different composite materials are all being considered as alternatives to carbonaceous materials with limited performance [9–11].

Graphene, a two-dimensional honeycomb lattice of $sp^2$-bonded carbon atoms, has emerged to be an exciting material with numerous potential applications. An exciting feature of graphene is its unique electronic structure that exhibits linear dispersion at a high symmetry point in the reciprocal space, resulting in effective dynamics of electrons thereby behaving like a Dirac solid [12,13]. More recently, the development of supercapacitors device has been concentrated on graphene due to its theoretical high surface area (2630 $m^2g^{-1}$), high electrical conductivity, chemical stability and excellent mechanical properties [14–19]. Graphene also offers a suitable platform for accommodating metal oxide materials or conducting polymers for energy storage applications [20,21]. This is usually attributed to the large surface area of graphene which allows for uniform loading and incorporation of these materials.

Recently, several groups have demonstrated the integration of manganese oxide ($MnO_2$) on graphene as electrode for capacitive storage application. $MnO_2$ is a transition metal oxide that has attracted much attention as electrode due to its multiple reversible electrochemical reaction, natural abundance, low cost, and environmental compatibility [22–24]. For example, Yong-Qing Zhao *et al* recently reported a composite of $MnO_2$/graphene/nickel foam using a facile electrochemical deposition strategy [25]. Several studies have attempted to synthesize various graphene/$MnO_2$ nanocomposite using techniques such as chemical [26 27], microwave irradiation [28],

electrodeposition [29–31], redox deposition [32] and polymer-assisted chemical reduction [33]. However, most of the synthesis routes make use of concentrated acid, strong reducing agents such as hydrazine ($N_2H_4$) and sodium borohydride ($NaBH_4$) which distort the $sp^2$ honey comb lattice of the graphene leading to very high defective samples and inferior electronic properties. Synthesizing a three dimensional defect free composite of graphene-$MnO_2$ with very good porosity and conductivity would be considered a step forward in the development of composite materials for electrochemical energy storage technology.

In this work, we present a simple green and very efficient approach to fabricate novel nickel foam-Graphene/Manganese oxide (NF-G/$MnO_2$) composite. We also explore the potential of the NF-G/$MnO_2$ composite as an electrode for high performance supercapacitor applications. The NF-G/$MnO_2$ composite has a high electrochemical surface area and 3D porous interconnected network. The $MnO_2$ deposited by the microwave technique exhibited a flower-like structure uniformly anchored on 3D porous nickel foam-Graphene. The unique electrode structure not only boosted ion and electron exchange in electrochemical processes but also serve as a 3D platform for combination and integration of $MnO_2$ on the NF-G. The composites (NF-G/$MnO_2$) displayed good electrochemical behavior with good capacitance retention at high current density. Our results showed that NF-G provides a suitable platform for developing functional materials with enhanced electrochemical performance.

## 2. Experimental

Synthesis of Graphene on nickel foam was done using chemical vapour deposition (CVD). The nickel foam serves as a template for the growth [34]. Nickel foams (Alantum innovation in alloy foam Munich Germany, 420 g $m^{-2}$ in area density and 1.6 mm in thickness) were used as the template. The nickel foam was annealed at 800 $^{o}$C in the presence of Ar and $H_2$ for 20 min to remove any form of impurities present in the foam, before the introduction of the $CH_4$ gas at the

temperature of 1000 $^{o}$C. The flow rates of the gases $CH_4$:$H_2$: Ar were 10 sccm: 200 sccm: 300 sccm. After 10 minutes of deposition, the sample was rapidly cooled by pushing the quartz tube to a lower temperature region. NF-G/$MnO_2$ composite was synthesized by in-situ hydrothermal reduction method using microwave irradiation. Originally, NF-G was immersed in 10 $cm^3$ of 0.02 M of $KMnO_4$ (Merck). The mixture was then transferred into a quartz vessel in a microwave reactor (Anton Paar Synthos 3000 multimode reactor, 1400 W magnetron power) equipped with a wireless pressure and temperature sensor. The reactor was operated in the pressure mode using a power of 400 W; the sample temperature was ramped at 10 $^{o}$C/min to 110 °C and kept constant at this temperature for 2 hours, ramp/hold time was 11/120 minutes while the pressure was maintained at 80 bars throughout the hold period. After cooling the reaction chamber to room temperature, the sample was repeatedly washed with deionized water to remove traces or excess of undeposited $MnO_2$. Finally, samples were dried at 60 °C in an electric oven. After drying, the NF-G/$MnO_2$ composite was tested as electrode for electrochemical capacitor. To estimate the mass of graphene and $MnO_2$ in the composite, we take note of the mass of materials after each step of the experiment to obtain the NF-G/$MnO_2$. Typical the NF-G/$MnO_2$ composite contains 72 wt.% $MnO_2$ and 28 wt.% graphene.

### 2.1. Characterization of the samples

The Raman spectra of NF-G and NF-G/$MnO_2$ composite were recorded using a WITEC-alpha 300R+ confocal Raman spectrometer (WITEC GmbH). The excitation source was the 532-nm laser (2.33 eV) through a numerical aperture of 0.9 and 100x magnification. Powder X-ray diffraction (XRD) was recorded using an (XPERT-PRO diffractometer PANalytical BV, Netherlands) with theta/theta geometry. Qualitative phase analysis of samples was conducted using the X'pert Highscore search match software. The surface morphology and microstructure of the composite was investigated using the high resolution Zeiss Ultra plus 55 Field emission scanning electron microscope (FE-SEM) operated at 2.0 kV. Transmission electron microscopy (TEM) images were obtained on a JEOL JEM-2100F microscope operated at 200 kV

The electrochemical properties of the supercapacitor electrodes were studied in a three-electrode configuration system using an Autolab PGSTAT workstation 302 (ECO-CHEMIE) driven by the GPES software. The as-prepared NF-G/$MnO_2$ served as the working electrode, glassy carbon plate as the counter electrode and Ag/AgCl (3 M KCl) served as the reference electrode and 1 M $Na_2SO_4$ was used as the electrolyte. Electrochemical impedance spectroscopy (EIS) was performed in the frequency range of 100 kHz-10 mHz.

## 3. Results and discussion

The microwave technology has been known to reduce reaction times and increase productivity of materials compared to other conventional available techniques. This technology makes use of two heating mechanisms namely dipolar polarization and ionic conduction. The dipoles in the reaction chamber are involved in the polarization effect, while the charged particles in a reaction chamber (usually ions) contribute to ionic conduction effect [35]. When reaction chamber is irradiated, the dipoles or ions in the sample align themselves in the direction of applied electric field. When the applied field oscillates, the dipole or ion field realigns itself with the alternating electric field thereby losing energy in the form of heat through friction and dielectric loss [36]. The microwave irradiation induces a volumetric heating by direct coupling of microwave energy with the molecules that are present in the reaction chamber. This increases the temperature of the whole liquid volume in the chamber simultaneously, compared with conventionally heating system, where the reaction chamber in contact with the hot vessel walls is heated first [36,37]. Figure 1 shows the schematic illustration for the fabrication process of NF-G/$MnO_2$. The formation of the $MnO_2$ flower-like structure on NF-G forms as follows: Since microwave-enhanced irradiation is based on efficient interaction of molecules with the electromagnetic waves, the electromagnetic waves couple directly with the molecules of potassium permanganate ($KMnO_4$) in the entire reaction vessel. This leads to a rapid rise in temperature and formation of large amount of nuclei in a short time converting aqueous permanganate ($MnO_4^-$) to $MnO_2$, which is followed by self-assembly of amorphous spheres. Since this process is not limited by the thermal conductivity, but Ostwald ripening process

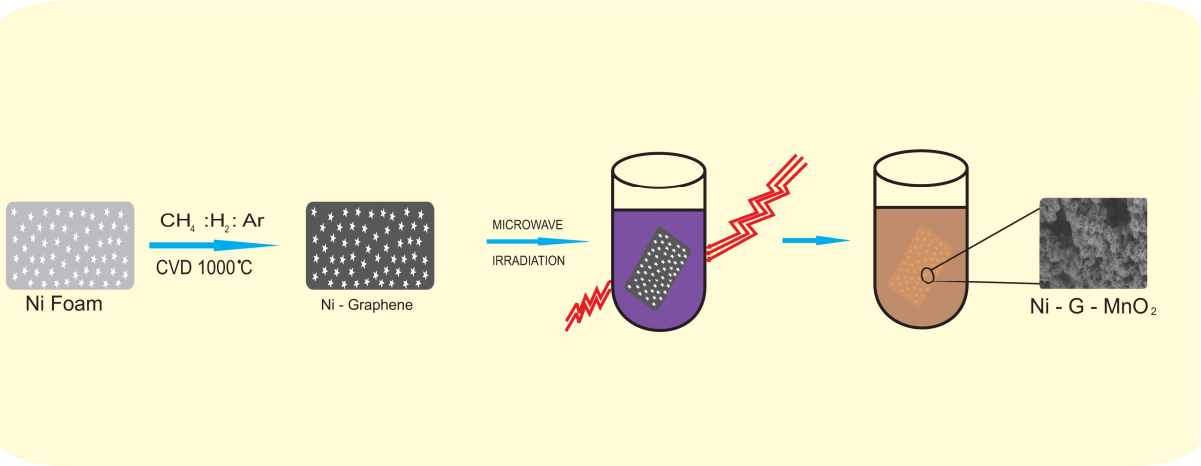


**Figure 1** Schematic illustration for the formation process of Nickel foam-graphene/$MnO_2$ composite (NF-G/$MnO_2$).

also occurs. In brief smaller particles dissociates while the bigger ones grow into sheet like particles with a lamellar structure, these sheet-like particles tend to curl and assemble forming the flower-like structure [38]. Under a neutral pH condition, the reaction between carbon (graphene) and $KMnO_4$ is also governed by the following equation [39]:

$$4\,MnO_4^- + 3C + H_2O \rightarrow 4MnO_2 + CO_3^{2-} + 2HCO_3^- \qquad (1)$$

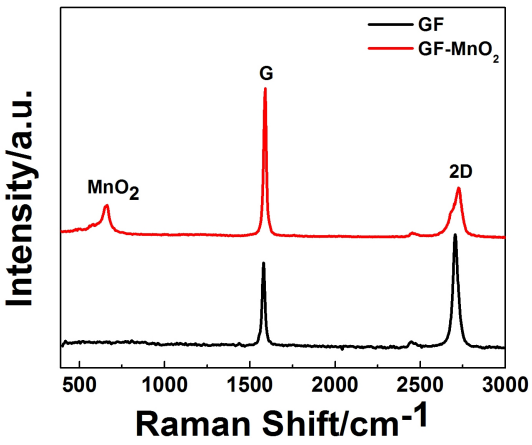


**Figure 2** Raman spectra of (a) Nickel foam graphene (b) Nickel foam-graphene/$MnO_2$ composite (NF-G/$MnO_2$).

Figure 2 shows the Raman spectrum of the graphene on the nickel foam which consists of two major peaks at 1580 $cm^{-1}$ and 2704 $cm^{-1}$. These peaks correspond to the G and 2D modes of graphene. The intensity of the 2D, the $I_{2D}/I_G$ ratio and the FWHM of 38.8 $cm^{-1}$ indicated that

graphene consist of mostly few layers. The absence of the D-peak (disorder) at 1350 $cm^{-1}$ shows that our graphene is of good quality and low defect density[40]. The Raman spectrum of NF-G/$MnO_2$ composite showed an additional sharp peak at 649.9 $cm^{-1}$ which evidences the deposition of $MnO_2$ on the graphene foam. This peak and belongs to the $A_g$ mode arising from breathing vibrations of $MnO_6$ octahedral double chains. It also corresponds to the Mn-O stretching vibration mode in the basal plane of $MnO_6$ octahedral chains [41]. The well-defined Raman spectrum reflects the good crystallinity of the $MnO_2$ in the composite material. The observed reduction of the 2D peak intensity with respect to G peak is a clear indication of incorporation of $MnO_2$ as impurity to graphene foam which is due to the interaction of the graphene with $MnO_2$ [42].

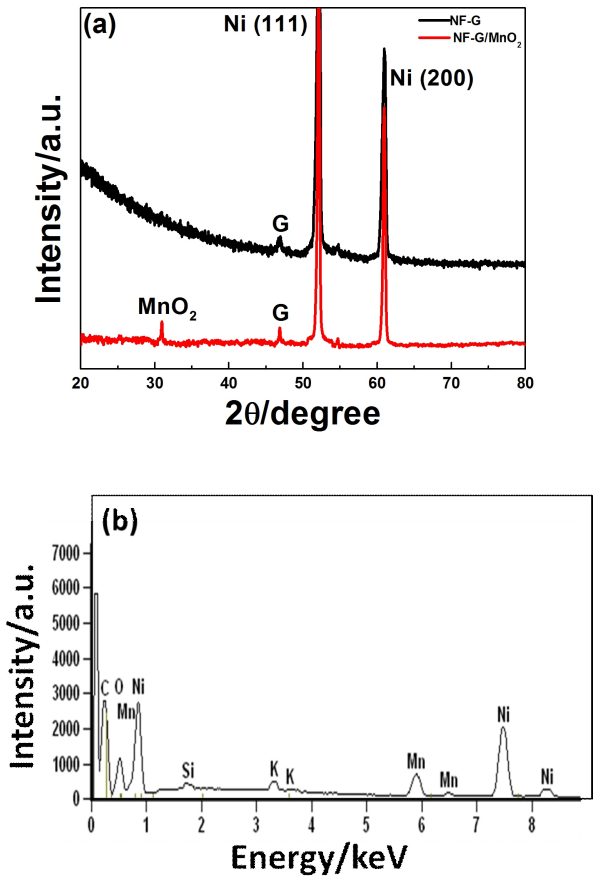


**Figure 3 (a)** XRD patterns of Nickel foam graphene and Nickel foam-graphene/$MnO_2$ composite (b) EDX pattern of Nickel foam-graphene/$MnO_2$

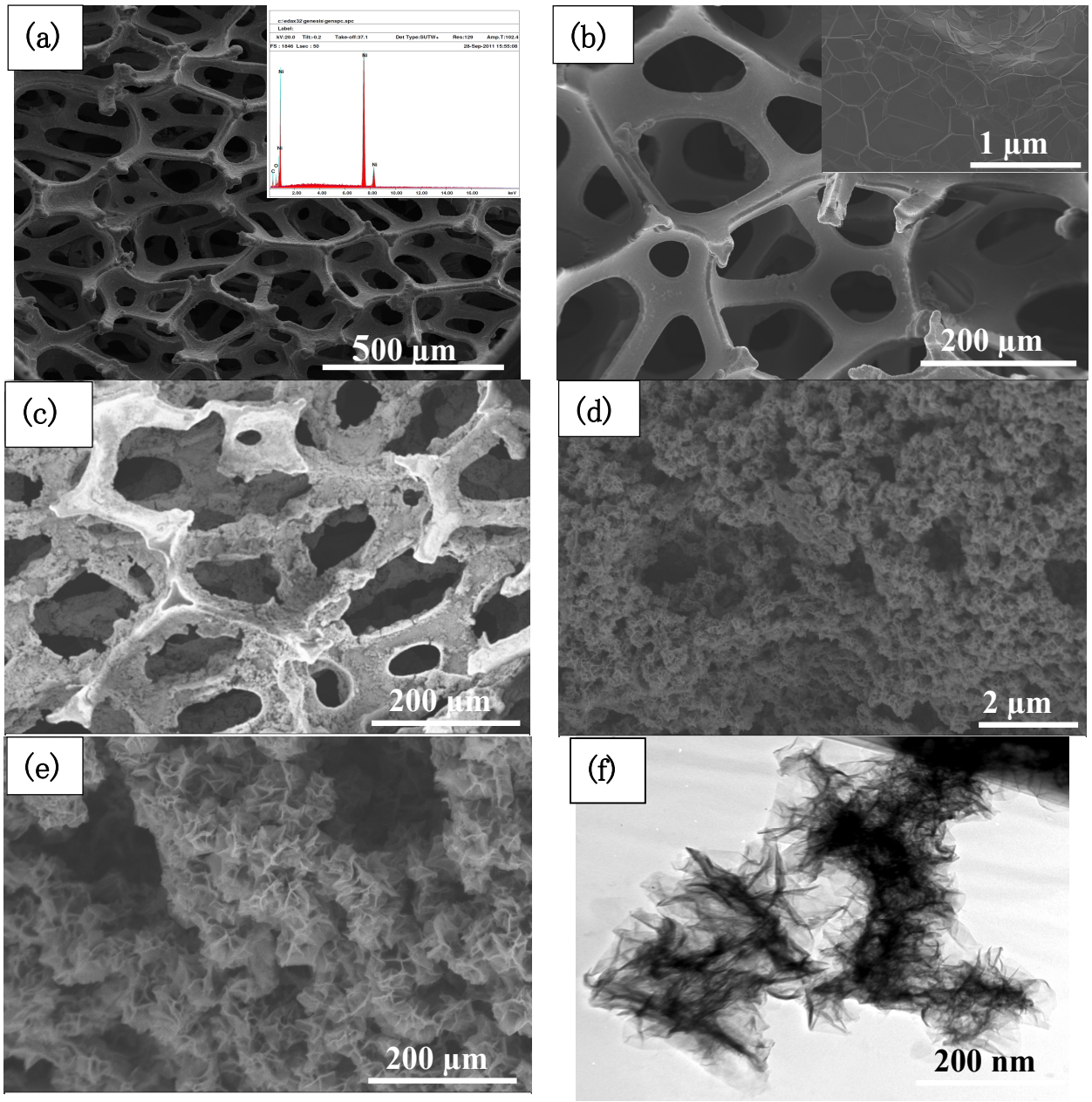


**Figure 4** SEM micrographs of (a, b) Nickel foam-Graphene (NF-G) at different magnifications, (c, d, e) Nickel foam-Graphene coated with $MnO_2$ (NF-G/$MnO_2$) at different magnifications and 4 (f) TEM of the graphene foam/$MnO_2$ composite.

The crystallographic structure of the composite was determined by XRD. Figure 3 shows XRD patterns of NF-G and NF-G/$MnO_2$. The two very strong XRD peaks recorded at 52.1° and 60.9° originate from Ni and could be assigned to the (111), (200) phase of nickel. The diffraction peak of the $MnO_2$ on NF-G is broad with very low intensity signal resulting from small average crystallite domain size of $MnO_2$. The low intensity peaks is due to the fact that very strong signal intensities

peaks originating from nickel foam overlaps and suppress that of graphene and $MnO_2$. Figure 3 (b) is the EDX of the sample which shows the presence of manganese in the sample with little traces of potassium which likely comes from unreacted or residual $KMnO_4$ used as $MnO_2$ precursor.

Figure 4 (a) shows the FE-SEM micrograph of the nickel foam alone exhibiting three-dimensional porous network. Inset to the figure is the EDX spectra of the NF which shows elemental composition of the foam revealing the presence of nickel. Figure 4 (b) shows the image of graphene on the nickel foam. The graphene grows on the template material (NF) mimicking the three-dimensional porous network structure of the nickel-foam. Inset to this figure is the high magnification which shows the presence of graphene. It reveals that the graphene consists of wrinkles and ripples which is due to the different thermal expansion coefficients of Ni and graphene during the CVD synthesis [43]. This structure can be an excellent substrate for incorporation of oxide materials for electrochemical applications. Figure 4 (c, d and e) show FE-SEM micrographs of NF-G/$MnO_2$ at different magnifications. It can be seen that the $MnO_2$ particles uniformly coat the whole surface of the NF-G thus exhibiting a porous and continuous electroconducting network structure. This unique structure or morphology makes it useful in electrochemical capacitors when ions are adsorbed onto the surface of the samples thereby leading to improved capacitance behavior. It also provides a very good electrode-electrolyte interface for exchange of ions from the electrolyte. Figure 4 (d) reveals a high dense nanostructure of $MnO_2$ anchored onto the NF-G surface, while figure 4 (e) shows that the nanostructured $MnO_2$ has a flower like structure that was formed by the self-assembly of nanosheets during the synthesis process [44]. Figure 4 (f) presents TEM images of NF-G/$MnO_2$ composite confirming the porous nature of the flower-like nanostructure shown in the SEM images.

Figure 5 (a) compares the CV of the NF and NF-G at a scan rate of 10 mV $s^{-1}$ and it can be clearly seen that the capacitance performance of the NF is negligible when compared with that of the NF-G. The CV of NF-G shows two redox peaks due to the $Ni^{2+}/Ni^{3+}$ redox process arising from the nickel foam [45]. Figure 5 (b) shows the discharge curve of NF-G at a current density of 1 A $g^{-1}$ the curve

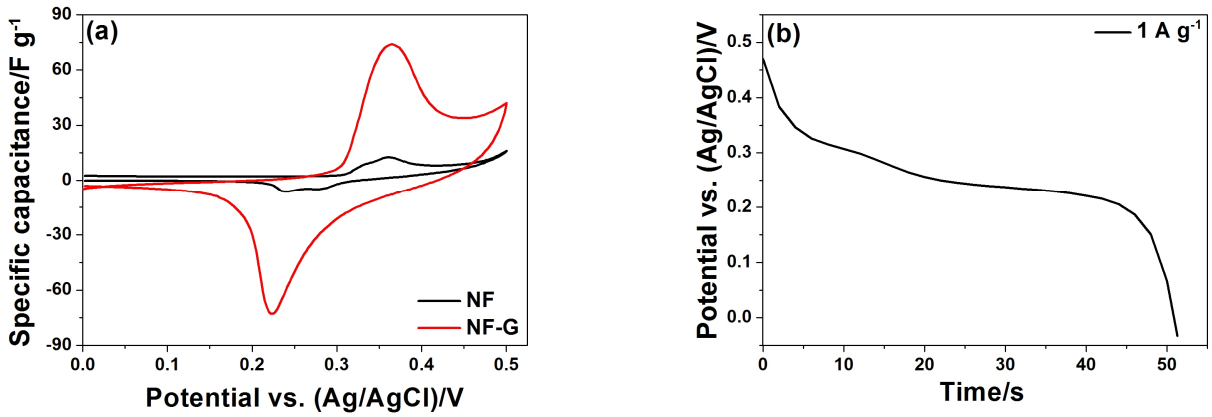


**Figure 5** (a) Cyclic voltammetry curves of NF and NF-G composite at scan rate of 10 mV $s^{-1}$ (b) the discharge curve of NF-G at a current density of 1 A $g^{-1}$.

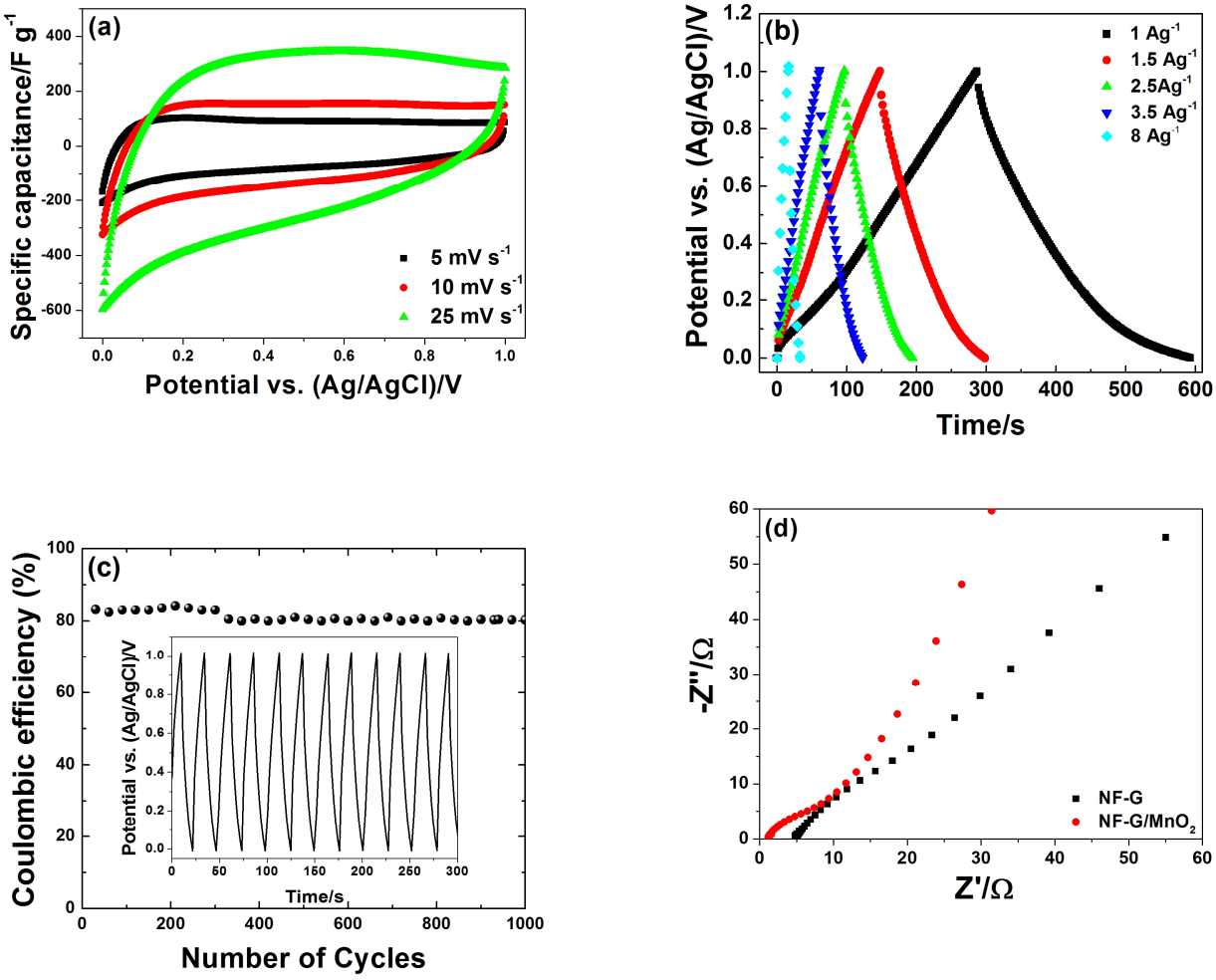


**Figure 6** Electrochemical results for NF-G/$MnO_2$ composite. (a) Cyclic voltammetry curves of NF-G/$MnO_2$ composite measured at different scan rates, (b) the galvanostatic charge-discharge curve at different current densities, (c) the Coulombic efficiency of the composite at a current density of 2.5 A $g^{-1}$, (the inset to the figure shows the continuous charge-discharge curve) and (d) EIS plot of both NF-G and NF-G/$MnO_2$.

displays a non-linear behavior indicating a pseudocapacitive effect. Figure 6 (a) shows the NF-G/$MnO_2$ CV curves at different scan rates, showing a relatively rectangular shape, which is a characteristic of an ideal capacitive behavior. The distortions from a perfect rectangular geometry demonstrate pseudocapacitive effects and contribution from $MnO_2$. The figure also indicated that the composite electrodes exhibits good electrochemical reversibility between 0 and 1 V. Figure 6 (b) shows the galvanostatic charge-discharge curves of the NF-G/$MnO_2$ composite at different current densities. It can be observed that the NF-G/$MnO_2$ curves are almost linear and symmetrical, which is a typical characteristic of an ideal capacitor behavior. The specific capacitance ($C_s$) and Coulombic efficiency (ε also referred to as Faradaic or current efficiency) values were calculated from the charge-discharge curve using the following equations:

$$C_s = \frac{i \times \Delta T}{\Delta V \times m} \tag{2}$$

$$\varepsilon = \frac{\Delta t_{discharge}}{\Delta t_{charge}} \times 100\% \tag{3}$$

where i is the current applied, $\Delta T$ is the discharge time and $\Delta V$ is voltage applied, m is the mass of active electrode material. Specific capacitances values of 305, 226, 222 and 211 F $g^{-1}$ were obtained at a current density of 1, 1.5, 2.5 and 3.5 A $g^{-1}$. The specific capacitance value in this present work is low compared to the values reported by Yong-Qing Zhao et al [25], this may be due presence of potassium or other impurities in composite which may limit the redox efficiency. An optimum, impurity-free composite should give higher capacitance. However, here we have been able to demonstrate the feasibility of using nickel foam as a direct template for synthesis of 3D conducting porous graphene and subsequently loading it with crystalline $MnO_2$ rather than going through the process of chemical method for production of graphene oxide before finally reducing to the graphene which normally introduces defects in the samples and often leads to inferior electronic properties.

Figure 6 (c) shows that the galvanostatic cycling performance of the composite was found to be stable, with cycle efficiency (Coulombic efficiency) of about 80 % for 1000 charge/discharge cycles

which demonstrate the excellent stability and performance of the electrode. The improved electrochemical performance of NF-G/$MnO_2$ as compared to NF-G, is due to the synergistic effect between graphene and $MnO_2$ leading to improved conductivity of the composite. Also the 3D porous network structure of the nickel foam helps to provide easy access to ions from the electrolyte at the electrode/electrolyte interface.

The electrochemical impedance spectroscopy (Nyquist) plot of NF-G and NF-G/$MnO_2$ is shown in figure 6 (d). It is a representation of the real and imaginary part of the impedance of the electrode material. It is worth stating that for ideal supercapacitors, the Nyquist plot should be a line perpendicular to the real axis at low frequency. From the Nyquist plot of NF-G/$MnO_2$ we observe that it is much closer to the ideal behavior which might be attributed to the low charge transfer of graphene and $MnO_2$; thus indicating a better capacitive behavior.

## 4. Conclusions

This work has demonstrated the possibility of using hydrothermal microwave irradiation in synthesis of novel functional materials for high performance electrochemical applications. NF-G was synthesized using chemical vapor deposition (CVD). The 3D porous network structure of the NF-G allows for a uniform coating and efficient loading of $MnO_2$ through the hydrothermal microwave irradiation to form NF-G/$MnO_2$ composite. Raman spectroscopy, SEM and TEM reveal that high quality and defect free samples were synthesized by CVD system. Electrochemical investigation indicated that the NF-G/$MnO_2$ had a maximum capacitance of 305 F $g^{-1}$. The uniform adsorption of $MnO_2$ nanostructures onto the surface of NF-G provides a much larger surface area for reaction during electrochemical process, leading to the effective utilization of the electrode material. The electrode material also exhibits excellent performance and rate capability which is due to efficient charge transfer and ion diffusion in the porous network of the composite. The work shows that pseudocapacitance can be effectively loaded onto the surface of NF-G via microwave irradiation and has potential for high performance supercapacitor application.

**Acknowledgements**

This work is based upon research supported by the South African Research Chairs Initiative of the Department of Science and Technology (SARCHi-DST) and the National Research Foundation (NRF). Any opinion, findings and conclusions or recommendations expressed in this work are those of authors and therefore the NRF and DST do not accept any liability with regard thereto. A. Bello, M. Fabiane, and O.O. Fashedemi acknowledge financial support from University of Pretoria and NRF for PhD bursaries.

**References**

[1] B.E. Conway, Electrochemical supercapacitors scientific fundamentals and technological applications 1999.

[2] R. Kötz, Principles and applications of electrochemical capacitors, Electrochimica Acta. 45 (2000) 2483–2498.

[3] X. Zhao, B.M. Sánchez, P.J. Dobson, P.S. Grant, The role of nanomaterials in redox-based supercapacitors for next generation energy storage devices, Nanoscale. 3 (2011) 839–855.

[4] P.J. Hall, M. Mirzaeian, S.I. Fletcher, F.B. Sillars, A.J.R. Rennie, G.O. Shitta-Bey, G. Wilson, A. Cruden, R. Carter, Energy storage in electrochemical capacitors: designing functional materials to improve performance, Energy Environmental Science. 3 (2010) 1238-1251.

[5] E. Frackowiak, Carbon materials for supercapacitor application, Physical Chemistry Chemical Physics 9 (2007) 1774–1785.

[6] A. Burke, R&D considerations for the performance and application of electrochemical capacitors, Electrochimica Acta. 53 (2007) 1083–1091.

[7] E. Frackowiak, F. Béguin, Carbon materials for the electrochemical storage of energy in capacitors, Carbon 39 (2001) 937–950.

[8] D. Villers, D. Jobin, C. Soucy, D. Cossement, R. Chahine, L. Breau and D. Be´langer, The influence of the range of electroactivity and capacitance of conducting polymers on the performance of carbon conducting polymer hybrid supercapacitor, Journal of The Electrochemical Society. 150 (2003) A747-A752.

[9] F. Fusalba, H.A. Ho, L. Breau, D. Be, Poly(cyano-substituted diheteroareneethylene) as active electrode material for electrochemical supercapacitors, Chemistry of Materials 12 (2000) 2581–2589.

[10] P. Simon, Y. Gogotsi, Materials for electrochemical capacitors, Nature Materials 7 (2008) 845–854.

[11] L.L. Zhang, X.S. Zhao, Carbon-based materials as supercapacitor electrodes, Chemical Society Reviews 38 (2009) 2520–2531.

[12] A.K. Geim, K.S. Novoselov, The rise of graphene, Nature Materials (2007) 183–191.

[13] K.S. Novoselov, A.K. Geim, S.V. Morozov, D. Jiang, M.I. Katsnelson, I.V. Grigorieva, S.V. Dubonos, A.A. Firsov, Two-dimensional gas of massless Dirac fermions in graphene, Nature 438 (2005) 197–200.

[14] K.S. Novoselov, A.K. Geim, S. Morozov, Electric field effect in atomically thin carbon films, Science 306 (2004) 666–669.

[15] M.D. Stoller, S. Park, Y. Zhu, J. An, R.S. Ruoff, Graphene-based ultracapacitors, Nano Letters. 8 (2008) 3498–3502.

[16] Y. Wang, Z. Shi, Y. Huang, Y. Ma, C. Wang, M. Chen and Y.S. Chen, Supercapacitor devices based on graphene materials, Journal of Physical Chemistry C. 113 (2009) 13103–13107.

[17] C. Liu, Z. Yu, D. Neff, A. Zhamu, B.Z. Jang, Graphene-based supercapacitor with an ultrahigh energy density, Nano Letters 10 (2010) 4863–4868.

[18] Y. Zhu, S. Murali, W. Cai, X. Li, Graphene and graphene oxide: synthesis, properties, and applications, Advanced Materials 22 (2010) 3906–3924.

[19] Y. Sun, Q. Wu, G. Shi, Graphene based new energy materials, Energy & Environmental Science. 4 (2011) 1113-1132.

[20] S. Guo, S. Dong, Graphene nanosheet: synthesis, molecular engineering, thin film, hybrids, and energy and analytical applications, Chemical Society Reviews 40 (2011) 2644–72.

[21] T.Y. Kim, H.W. Lee, M.D. Stoller, D.R. Dreyer, C. W Bielawski., R.S. Ruoff and K.S. Suh, High-performance supercapacitors based on poly(ionic liquid)-modified graphene electrodes, ACS Nano 5 (2011) 436–442.

[22] X. Zhang, X. Sun, Y. Chen, D. Zhang, Y. Ma, One-step solvothermal synthesis of graphene/$Mn_3O_4$ nanocomposites and their electrochemical properties for supercapacitors, Materials Letters 68 (2012) 336–339.

[23] W. Wei, X. Cui, W. Chen, D.G. Ivey, Manganese oxide-based materials as electrochemical supercapacitor electrodes, Chemical Society Reviews 40 (2011) 1697–1721.

[24] J. Liu, J. Essner, J. Li, Hybrid supercapacitor based on coaxially coated manganese oxide on vertically aligned carbon nanofiber arrays, Chemistry of Materials 22 (2010) 5022–5030.

[25] Y-Q. Zhao, D-D. Zhao, P-Y. Tang, Y-M. Wang, C-L. Xu, H-L. Li, $MnO_2$/graphene/nickel foam composite as high performance supercapacitor electrode via a facile electrochemical deposition strategy, Materials Letters 76 (2012) 127–130.

[26] S. Chen, J. Zhu, X. Wu, Q. Han, X. Wang, Graphene oxide−$MnO_2$ nanocomposites for supercapacitors, ACS Nano 4 (2010) 2822–2830.

[27] Y. Chen, Y. Zhang, D. Geng, R. Li, H. Hong, J. Chen, X. Sun, One-pot synthesis of $MnO_2$/graphene/carbon nanotube hybrid by chemical method, Carbon 49 (2011) 4434–4442.

[28] J. Yan, Z. Fan, T. Wei, W. Qian, M. Zhang, F. Wei, Fast and reversible surface redox reaction of graphene–$MnO_2$ composites as supercapacitor electrodes, Carbon 48 (2010) 3825–3833.

[29] H. Gao, F. Xiao, C.B. Ching, H. Duan, High-performance asymmetric supercapacitor based on graphene hydrogel and nanostructured $MnO_2$, ACS Applied Materials and Interfaces 4 (2012) 2801–2810.

[30] G. Yu, L. Hu, M. Vosgueritchian, H. Wang, X. Xie, J. R. McDonough, X. Cui, Y. Cui, Z. Bao, Solution-processed graphene/$MnO_2$ nanostructured textiles for high-performance electrochemical capacitors, Nano Letters 11 (2011) 2905–2911.

[31] Q. Cheng, J. Tang, J. Ma, H. Zhang, N. Shinya, L-C. Qin, Graphene and nanostructured $MnO_2$ composite electrodes for supercapacitors, Carbon 49 (2011) 2917–2925.

[32] Z. Li, J. Wang, S. Liu, X. Liu, S. Yang, Synthesis of hydrothermally reduced graphene/$MnO_2$ composites and their electrochemical properties as supercapacitors, Journal of Power Sources 196 (2011) 8160–8165.

[33] Y. Qian, S. Lu, F. Gao, Preparation of $MnO_2$/graphene composite as electrode material for supercapacitors, Journal of Materials Science. 46 (2011) 3517–3522.

[34] A. Bello, K. Makgopa, M. Fabiane, D. Dodoo-Ahrin, K.I. Ozoemena, N. Manyala, Chemical adsorption of NiO nanostructures on nickel foam-graphene for supercapacitor applications, Journal of Material Science (2013) 48:6707–6712.

[35] M. Baghbanzadeh, L. Carbone, P.D. Cozzoli, C.O. Kappe, Microwave-assisted synthesis of colloidal inorganic nanocrystals, Angewandte Chemie 50 (2011) 11312–11359.

[36] C. Oliver Kappe, Microwave dielectric heating in synthetic organic chemistry, Chemical Society Reviews 37 (2008) 1127–1139.

[37] C.O. Kappe, How to measure reaction temperature in microwave-heated transformations, Chemical Society Reviews 42 (2013) 4977–4990.

[38] Y. Li, J. Wang, Y. Zhang, M. N. Banis, J. Liu, D. Geng, R. Li, X. Sun, Facile controlled synthesis and growth mechanisms of flower-like and tubular $MnO_2$ nanostructures by microwave-assisted hydrothermal method, Journal of Colloid and Interface Science 369 (2012) 123–128.

[39] X. Jin, W. Zhou, S. Zhang, G.Z. Chen, Nanoscale microelectrochemical cells on carbon nanotubes, Small 3 (2007) 1513–1517.

[40] A.C. Ferrari, Raman spectroscopy of graphene and graphite: disorder, electron–phonon coupling, doping and nonadiabatic effects, Solid State Communications 143 (2007) 47–57.

[41] T. Gao, H. Fjellvåg, P. Norby, A comparison study on Raman scattering properties of α- and β-$MnO_2$, Analytica Chimica Acta 648 (2009) 235–239.

[42] Z. Ni, T. Yu, Z. Luo, Y. Wang, L. Liu, Probing charged impurities in suspended graphene using Raman spectroscopy, ACS Nano 3 (2009) 569–574.

[43] S.J. Chae, F. Gunes, K.K. Kim, E.S. Kim, G.H. Han, S.M. Kim, H-J. Shin, S-M. Yoon, J-Y Choi, M.H. Park, C.W. Yang, D. Pribat, Y.H. Lee, Synthesis of large-area graphene layers on poly-nickel substrate by chemical vapor deposition: wrinkle formation, Advanced Materials 21 (2009) 2328–2333.

[44] H. Chen, J. He, C. Zhang, H. He, Self-assembly of novel mesoporous manganese oxide nanostructures and their application in oxidative decomposition of formaldehyde, Journal of Physical Chemistry C 111 (2007) 18033–18038.

[45] L-R. Zhang, J. Zhao, M. Li, H-T. Ni, J-L. Zhang, X-M. Feng, Y-W. Ma, Q-L. Fan, X-Z. Wang, Z. Hu, W. Huang, Preparation of graphene supported nickel nanoparticles and their application to methanol electrooxidation in alkaline medium, New Journal of Chemistry 36 (2012) 1108-1113.